Wind and Structures, Vol. 5, No. 6 (2002) 479-492
DOI: http://dx.doi.org/10.12989/was.2002.5.6.479

Time domain flutter analysis of the Great Belt East Bridge

Lamberto Briseghella[†] and Paolo Franchetti[‡]

Università di Padova, Padova, Italy

Stefano Secchi[‡†]

LADSEB-CNR Padova, Italy

(Received February 15, 2000, Revised April 24, 2000, Accepted March 15, 2001)

Abstract. A finite element aerodynamic model that can be used to analyse flutter instability of long span bridges in the time domain is presented. This approach adopts a simplified quasi-steady formulation of the wind forces neglecting the vortex shedding effects. The governing equations used are effective only for reduced velocities V^* sufficiently great: this is generally acceptable for long-span suspension bridges and, then, the dependence of the wind forces expressions of the flutter derivatives can be neglected. The procedure describes the mechanical response in an accurate way, taking into account the non-linear geometry effects (large displacements and large strains) and considering also the compressed locked coil strands instability. The time-dependence of the inertia force due to fluid structure interaction is not considered. The numerical examples are performed on the three-dimensional finite element model of the Great Belt East Bridge (DK). A mode frequency analysis is carried out to validate the model and the results show good agreement with the experimental measurements of the full bridge aeroelastic model in the wind tunnel tests. Significant parameters affecting bridge response are introduced and accurately investigated.

Key words: flutter; FEM; aerodynamic.

1. Introduction

In the design of long-span suspension bridges the description of the aeroelastic behaviour is an interdisciplinary research subject of great topicality: it involves structural and aerodynamic problems and is decisive in influencing design choices. The aim of this paper is to study the behaviour of this type of structure subject to instability phenomena of the flutter type.

In the analysis the bridge was schematised by means of finite elements model and the aerodynamic actions are applied to the deck. This analysis was done in the time domain following an alternative procedure to the traditional one in the frequency domain (Scanlan 1996) and, in comparison, it shows the considerable advantage of a better physical description of the phenomenon. It also allows the effects of both the material and geometrical nonlinearities of the system to be considered.

† Professor of Structural Dynamics
‡ Structural Engineer
‡† Research Scientist

The description of the self-excited loads adopts a "quasi-static" formulation for the wind forces (Diana 1998), in which the relative motion between incident flow and deck is considered. These actions are function of both the time-history of the incident flow affecting the bridge and the motion of the bridge itself. Nevertheless, if the dynamic system formed by the bridge and the surrounding flow is assumed to be linear, the buffeting loads do not affect the motion stability (Li 1995). It is therefore possible, given the aims of the paper, to ignore the effect caused by aerodynamic turbulence.

2. Governing equations

A 3-D anticlockwise cartesian system is defined, in which the origin coincides with the centroid of the deck section, the axis *x* horizontal coincides with the longitudinal axis of the undeformed deck and the *y* and *z* axes, horizontal and vertical, respectively, are depicted in Fig. 1.

The quasi-static theory starts with the definition of the aerodynamic actions on a given section of deck in motion, the position of which on the bridge is identified by the longitudinal co-ordinate *x*: Fig. 1 shows that these actions depend on the interaction between incident flow and deck motion characteristics.

In the hypothesis of also considering the variability over time of the incident flow, the analytical equations of these actions, per unit length, result as :

$$\begin{aligned} F_D &= \frac{1}{2}\rho B C_D(\alpha) V_R^2, \\ F_L &= \frac{1}{2}\rho B C_L(\alpha) V_R^2, \\ M &= \frac{1}{2}\rho B^2 C_M(\alpha) V_R^2 \end{aligned} \tag{1}$$

$$F_y = -F_L \sin(\psi) + F_D \cos(\psi) \qquad F_z = F_L \cos(\psi) + F_D \sin(\psi) \tag{2}$$

$$\alpha = \theta - \psi \qquad V_R^2 = (W - \dot{z} + b_1\dot{\theta})^2 + (U - \dot{y})^2 \tag{3}$$

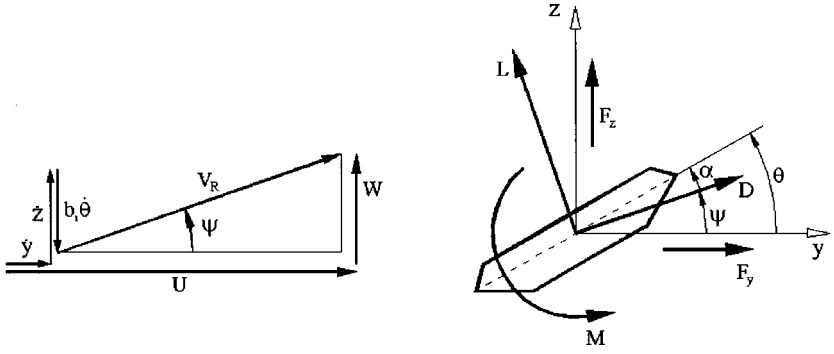

Fig. 1 Aerodynamic forces per unit length according to the quasi-static method for a deck section

where :

ρ is the air density;

B is the deck width;

$\boldsymbol{U}$, $\boldsymbol{W}$ represent the speed vectors of the flow in the horizontal and vertical direction, respectively.

V_R is the relative flow speed with respect to the section, expressed in vectorial form as:

$$\boldsymbol{V}_R = (\boldsymbol{U} + \boldsymbol{W}) - \boldsymbol{V}_P = \boldsymbol{V} - \boldsymbol{V}_P$$

where $\boldsymbol{V_P}$ is the speed of a point of the section. This value changes when the considered point P is varied. It is possible to refer to an equal relative speed for each point of the section if a particular point is taken for P set at a given distance b_1 from the rotational axis in a horizontal direction ;

ψ is the angle of the slope of the relative speed $\boldsymbol{V_R}$:

$$\psi = \arctan\left[\frac{(W - \dot{z} + \dot{\theta} b_1)}{(U - \dot{y})}\right] \tag{4}$$

α is the angle of attack of the incident flow with respect to the deck;

C_L, C_D, C_M are the static lift, drag and moment coefficients, measured as functions of the angle of attack α.

This formulation includes the nonlinear effects due to deck motion, those caused by wind turbulence and those generated by the variation of the aerodynamic coefficients with the actual angle of attack. The dependence is not considered of the aerodynamic coefficients of the reduced speed $V^* = (V_m / fB)$, where V_m is the absolute value of the average speed of the incident flow, f the frequency of the bridge motion and B the deck width: the application of Eqs. (1) and (2) is therefore limited only to the cases where V^* is high enough. This corresponds, in other words, to a situation in which the time taken by the flow to cross the section is much shorter than the oscillation period of the structure and of the period associated with the turbulence fluctuations: steady-state conditions are therefore approached and the angle Ψ (Fig. 1) is narrow, allowing easy treatment of the trigonometric equations.

The nonlinear discretised equations of the system motion can be written as :

$$\boldsymbol{M_s}\ddot{\boldsymbol{X}} + \boldsymbol{R_s}\dot{\boldsymbol{X}} + \boldsymbol{K_s}\boldsymbol{X} = \boldsymbol{F_a}(\boldsymbol{X}, \dot{\boldsymbol{X}}, \boldsymbol{V}(x, y, z, t)) + \boldsymbol{P} \tag{5}$$

$\boldsymbol{M_s}$, $\boldsymbol{R_s}$, $\boldsymbol{K_s}$ being the structural matrices of the bridge, $\boldsymbol{F_a}$ the vector of the aerodynamic forces that are generally nonlinear functions of the displacements $\boldsymbol{X}$ and velocity $\dot{\boldsymbol{X}}$, as well as of the space-time history of the turbulent wind $\boldsymbol{V}(x, y, z, t)$ of the incident flow, and $\boldsymbol{P}$ is the vector of the permanent loads considered.

Eq. (5) is nonlinear because of that nonlinear dependence of the aerodynamic forces of $\boldsymbol{X}$ and $\dot{\boldsymbol{X}}$; they also depend linearly on the coefficients of drag, torque and lift Eq. (1), in their turn, generally nonlinear functions of the wind angle of attack α.

These equations can only be solved numerically and their integration gives the displacements $\boldsymbol{X}$, velocities $\dot{\boldsymbol{X}}$ and accelerations $\ddot{\boldsymbol{X}}$ of the various nodal points of the model.

To simplify the formulation, Eq. (5) is linearised around the configuration of static equilibrium,

solving the problem:

$$\boldsymbol{K_s X_0} = \boldsymbol{F_a}(\boldsymbol{X}_0,\ \boldsymbol{0},\ \boldsymbol{V_m}) + \boldsymbol{P} \tag{6}$$

where the wind speed is assumed as constant and equal to the average value $\boldsymbol{V}_m$, of components U_m and W_m.

Once the solution $\boldsymbol{X}_0$ is obtained, the generalised aerodynamic forces $\boldsymbol{F_a}(\boldsymbol{X},\ \dot{\boldsymbol{X}},\ \boldsymbol{V}(x, y, z, t))$ are linearised around $\boldsymbol{X}_0$ from which the following equation is obtained :

$$\boldsymbol{F_a}(\boldsymbol{X}, \dot{\boldsymbol{X}}, \boldsymbol{V}(x, y, z, t)) \ = \ \boldsymbol{F_a}(\boldsymbol{X_0}, \boldsymbol{0}, \boldsymbol{V_m}) - \boldsymbol{K_{a0}}(\boldsymbol{X} - \boldsymbol{X_0}) - \boldsymbol{R_{a0}}\dot{\boldsymbol{X}} + \left.\frac{\partial \boldsymbol{F_a}}{\partial \boldsymbol{V}}\right|_{X_0} \Delta \boldsymbol{V} \tag{7}$$

given that :

$$\boldsymbol{K_{a0}} \ = \ \left.\frac{\partial \boldsymbol{F_a}}{\partial \boldsymbol{X}}\right|_{X_0} \tag{8a}$$

$$\boldsymbol{R_{a0}} \ = \ \left.\frac{\partial \boldsymbol{F_a}}{\partial \dot{\boldsymbol{X}}}\right|_{X_0} \tag{8b}$$

are the elastic and damping matrices, respectively, due to the field of aerodynamic forces evaluated for $\boldsymbol{V}(x, y, z, t) \equiv \boldsymbol{V}_m$, i.e., for an average speed, constant in space and time. It can be seen that the aeroelastic forces constitute a non-conservative field for the positional elements and a non-dissipative field for the velocity elements: these characteristics are highlighted by the non-symmetry of the matrices of aerodynamic stiffness (Eq. 8a) and damping (Eq. 8b).

Defining with :

$$\underline{\boldsymbol{X}} \ = \ \boldsymbol{X} - \boldsymbol{X}_0 \tag{9}$$

the disturbance around the position of static equilibrium defined by Eq. (6), Eq. (5) becomes, referring to Eq. (7) :

$$\boldsymbol{M_s}\ddot{\underline{\boldsymbol{X}}} + (\boldsymbol{R_s} + \boldsymbol{R_{a0}})\dot{\underline{\boldsymbol{X}}} + (\boldsymbol{K_s} + \boldsymbol{K_{a0}})\underline{\boldsymbol{X}} \ = \ \left.\frac{\partial \boldsymbol{F_a}}{\partial \boldsymbol{V}}\right|_{X_0} \Delta \boldsymbol{V} + \boldsymbol{P} \tag{10}$$

and, in the hypothesis of ignoring any form of aerodynamic turbulence :

$$\boldsymbol{M_s}\ddot{\underline{\boldsymbol{X}}} + (\boldsymbol{R_s} - \boldsymbol{R_{a0}})\dot{\underline{\boldsymbol{X}}} + (\boldsymbol{K_s} + \boldsymbol{K_{a0}})\underline{\boldsymbol{X}} = \boldsymbol{P} \tag{11}$$

Eq. (11) provides the motion of the bridge around the previously defined average value $\boldsymbol{X}_0$. The aerodynamic coefficients C_D, C_L and C_M are nonlinear functions of the angle of attack α. To simplify the calculation of $\boldsymbol{K_{a0}}$ and $\boldsymbol{R_{a0}}$, for the angles $|\alpha| < 5°$, the aerodynamic forces acting on the deck section can be linearised, that become, from Eq. (2) :

$$F_y = -F_L\sin(\psi) + F_D\cos(\psi) = \frac{1}{2}\rho B V_R^2[-C_L(\alpha)\sin(\psi) + C_D(\alpha)\cos(\psi)] \cong$$
$$\cong \frac{1}{2}\rho B U_m^2[-C_L(\alpha)\psi + C_D(\alpha)] \cong$$
$$\cong \frac{1}{2}\rho B U_m^2\left[-\left(\left.\frac{dC_L(\alpha)}{d\alpha}\right|_{\alpha_0}(\alpha-\alpha_0) + C_L(\alpha_0)\right)\psi + \left(\left.\frac{dC_D(\alpha)}{d\alpha}\right|_{\alpha_0}(\alpha-\alpha_0) + C_D(\alpha_0)\right)\right] \tag{12a}$$

$$F_z = F_L\cos(\psi) + F_D\sin(\psi) = \frac{1}{2}\rho B V_R^2[C_L(\alpha)\cos(\psi) + C_D(\alpha)\sin(\psi)] \cong$$
$$\cong \frac{1}{2}\rho B U_m^2[C_L(\alpha) + C_D(\alpha)\psi] \cong$$
$$\cong \frac{1}{2}\rho B U_m^2\left[\left.\frac{dC_L\alpha}{d\alpha}\right|_{\alpha_0}(\alpha-\alpha_0) + C_L(\alpha_0) + \left(\left.\frac{dC_D(\alpha)}{d\alpha}\right|_{\alpha_0}(\alpha-\alpha_0) + C_D(\alpha_0)\right)\psi\right] \tag{12b}$$

$$M = \frac{1}{2}\rho B^2 C_M(\alpha) V_R^2 \cong \frac{1}{2}\rho B^2 U_m^2\left[\left.\frac{dC_M(\alpha)}{d\alpha}\right|_{\alpha_0}(\alpha-\alpha_0) + C_M(\alpha_0)\right] \tag{12c}$$

where the single average horizontal component of the speed of incident flow is considered.

It is therefore possible to calculate the equations of the aerodynamic matrices according to Eq. (8), assuming for simplicity that

$$\alpha_0 = 0 \tag{13}$$

and substituting them in Eq. (11).

3. Model for three-dimensional flutter analysis

The bridge is schematised by means of a three-dimensional finite element model capable of describing the static and dynamic behaviour. Particular attention is paid to the modelling of the hangers and main cables on the suspension bridges and the stays on the cable-stay bridges to reproduce the acting static pre-load; it is also worthwhile predicting a nonlinear behaviour of the hangers and stays.

In order to simplify the implementation, further hypotheses are formulated as follows :

- only the horizontal component U of the flow velocity is considered, uniform and constant;
- the horizontal component of the deck motion velocity is ignored;
- $\alpha_0 = 0$ is just taken for an approximation of the aerodynamic forces.

In this way equations Eq. (12) become :

$$F_y \cong \frac{1}{2}\rho B U^2\left[-\left.\frac{dC_L}{d\alpha}\right|_0(\theta-\psi)\psi + C_{L0}\psi + C_{D0}\right] \cong \frac{1}{2}\rho B U^2\left[-C_{L0}\frac{\dot\theta b_1 - \dot z}{U} + C_{D0}\right] \tag{14a}$$

$$F_z \cong \frac{1}{2}\rho B U^2\left[\left.\frac{dC_L}{d\alpha}\right|_0(\theta-\psi) + C_{L0} + C_{D0}\psi\right] \cong \frac{1}{2}\rho B U^2\left[\left.\frac{dC_L}{d\alpha}\right|_0\left(\theta - \frac{\dot\theta b_1 - \dot z}{U}\right) + C_{L0} + C_{D0}\frac{\dot\theta b_1 - \dot z}{U}\right] \tag{14b}$$

$$M \cong \frac{1}{2}\rho B^2 U^2 \left[\left. \frac{dC_M}{d\alpha} \right|_0 (\theta - \psi) + C_{M0} \right] \cong \frac{1}{2}\rho B^2 U^2 \left[\left. \frac{dC_M}{d\alpha} \right|_0 \left(\theta - \frac{\dot{\theta} b_1 - \dot{z}}{U} \right) + C_{M0} \right] \tag{14c}$$

where a zero value of the derivative of the coefficient of drag calculated for $\alpha = 0$ is assumed, in accordance with the experimental observations for the common sections of the deck.

The actions of the wind are concentrated on a suitable number of nodes along the deck axis assuming that :

$$\begin{aligned} F_{y,N} &= F_y \Delta L_N \\ F_{z,N} &= F_z \Delta L_N \\ M_N &= M \Delta L_N \end{aligned} \tag{15}$$

where ΔL_N is the influence length of the load and N is the loaded node.

The calculation code used allows the definition of forcing actions dependent on the displacements of the d.o.f. of the system or on their velocities according to the following method :

$$\begin{aligned} &u_j = \{y; z; \theta\} \\ &P_i(u_j) = a_{ij} p(u_j) \qquad i, j = 1, 2, 3 \\ &Q_i(\dot{u}_j) = b_{ij} q(\dot{u}_j) \end{aligned} \tag{16}$$

where :

u_j is a component of the nodal displacement in the local system y, z, θ ;
$\dot{u}_j$ is a component of nodal velocity in the local system y, z, θ ;
a_{ij} , b_{ij} are scalar elements;
P_i , Q_i are the components of the forces and the moments in the directions y, z, θ ;
p, q are generic functions of u_j and $\dot{u}_j$.

The equations of the forces implemented in the code become :

$$F_{y,1,N} = a_{1y,N} f_{1y}(\dot{\theta}) = -\frac{1}{2}\rho B U b_1 \Delta L_N C_{L0} \dot{\theta} \qquad F_{y,3,N} = a_{3y,N} f_{3y} = \frac{1}{2}\rho B U^2 \Delta L_N C_{D0}$$

$$F_{y,2,N} = a_{2y,N} f_{2y}(\dot{z}) = \frac{1}{2}\rho B U \Delta L_N C_{L0} \dot{z}$$

$$F_{z,1,N} = a_{1z,N} f_1(\theta) = \frac{1}{2}\rho B U^2 \Delta L_N \left. \frac{dC_L}{d\alpha} \right|_0 \theta \qquad F_{z,4,N} = a_{4z,N} f_4 = \frac{1}{2}\rho B U^2 \Delta L_N C_{L0}$$

$$F_{z,2,N} = a_{2z,N} f_2(\dot{\theta}) = -\frac{1}{2}\rho B U b_1 \Delta L_N \left. \frac{dC_L}{d\alpha} \right|_0 \dot{\theta} \qquad F_{z,5,N} = F_{5z,N} f_5(\dot{\theta}) = \frac{1}{2}\rho B U b_1 \Delta L_N C_{D0} \dot{\theta}$$

$$F_{z,3,N} = a_{3z,N} f_3(\dot{z}) = \frac{1}{2}\rho B U \Delta L_N \left. \frac{dC_L}{d\alpha} \right|_0 \dot{z} \qquad F_{z,6,N} = a_{6z,N} f_6(\dot{z}) = -\frac{1}{2}\rho B U \Delta L_N C_{D0} \dot{z} \tag{17}$$

$$M_{1,N} = b_{1,N} g_1(\theta) = \frac{1}{2}\rho B^2 U^2 \Delta L_N \left. \frac{dC_M}{d\alpha} \right|_0 \theta \qquad M_{3,N} = b_{3,N} g_3(\dot{z}) = \frac{1}{2}\rho B^2 U \Delta L_N \left. \frac{dC_M}{d\alpha} \right|_0 \dot{z}$$

$$M_{2,N} = b_{2,N} g_2(\dot{\theta}) = -\frac{1}{2}\rho B^2 U b_1 \Delta L_N \left. \frac{dC_M}{d\alpha} \right|_0 \dot{\theta} \qquad M_{4,N} = b_{4,N} g_4 = \frac{1}{2}\rho B^2 U \Delta L_N C_{M0}$$

4. The East Belt Great Bridge

The above-described formulation was applied to the "East Belt Great Bridge" in Denmark, inaugurated on 14 June 1998. The total length of the bridge is 6790 m: the suspended central span is 1624 m, the height above sea level, 65 m and the two lateral spans, 535 m each; two lateral access viaducts 1567 m and 2529 m long, respectively, complete the bridge. It is the longest suspension bridge in Europe, second only in the world to the recently completed Akashi Kaikyo in Japan. It nevertheless holds the world record for span length, thanks to the orthotropic structure of the box girder with aerodynamic profile and the air spinning technique of main cables.

The main suspension system consists of two parallel cables erected 27 m spaced. They are supported by special steel saddles on top of the pylon; contained in a splay saddle at both ends of the deck and then anchored to anchor blocks.

The stiffening girder is suspended to two cables by means of double pairs of hangers set at a transversal interaxis of 27 m. This is rigid both flexure-wise and torsion-wise and has sections of equal transverse bulk for the entire length of the bridge. There are expansion joints at the anchor blocks at either end. The panels that form it are stiffened longitudinally by trapezoidal reinforcements 6 mm thick supported transversely by grid screens every 4 m. Next to the pylons the interaxis between the screens is reduced to 3 m. The deck is formed by 59 segments 48 m long, and in correspondence to the longitudinal distance between pairs of hangers, 24 m long.

Each main cable is constructed of 18648 high resistance steel wires of 5.38 mm diameter: the

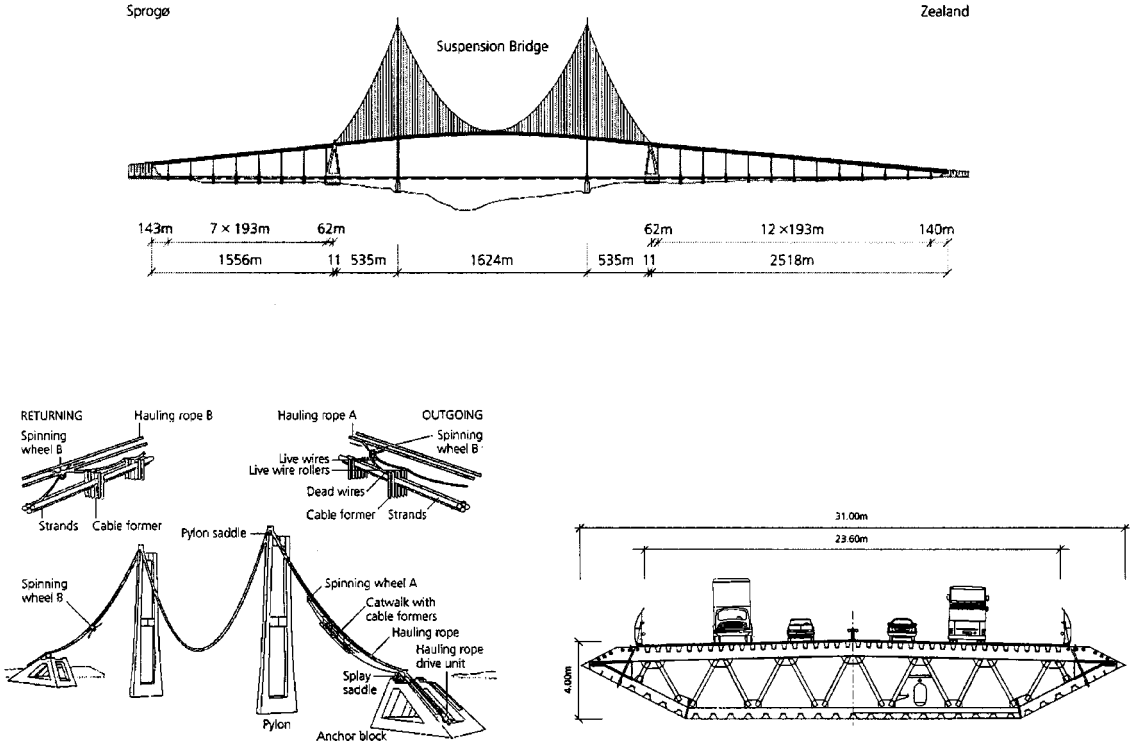

Fig. 2 Lateral, perspective and transversal section views of the bridge

total diameter is 827 mm. At the anchors the main cable is separated into 37 strands wound around a semicircular strand shoe. The latter are fastened to anchor blocks by pre-tensile bars embedded in concrete.

Each hanger consists of two locked-coil strands; each of these is made up of sockets and pre-pressed galvanised cables covered by HPDE extrusions (Rolla *et al*. 1997).

4.1. Description of the FEM model

The piers and towers were schematised with beam elements at 6 d.o.f. per node fixed to the base in correspondence to the foundation; the deck was modelled by a central beam, using beam elements without mass similar to the previous ones with inertia characteristics drawn from the analysis of a section of the type available in the project: the mass of the deck was schematised with concentrated masses that take into account the effective distribution. Other beam elements with infinite stiffness schematise the stiffening cross beams. Iso-resistant linear elastic behaviour was hypothesised for all these elements. An elastic module equal to 35 Gpa was assumed for the concrete material, while $E = 210$ Gpa was set for the steel. The hangers were schematised with 1 d.o.f. truss elements, not resistant to compression and linearly elastic to traction, with a module equal to 210 Gpa to model the behaviour of the cables. In total the mesh of the model was made up of 606 nodes and 938 beam elements (of which $106 \times 2 = 212$ truss elements). The extremity constraints reproduce the anchoring system to the ground. Table 1 summarises the basic frequencies obtained in the model for the static condition of its weight alone. Fig. 3 represents the corresponding modal forms.

At the same time a static check was done of the behaviour of the structure subject to the equivalent load given by the wind through the aerodynamic coefficients C_{D0}, C_{L0}, C_{M0}. The speed of incident flow was set at 38.9 m/s, i.e., the same as the design speed adopted for the structure. The distributed load was schematised with a series of concentrated nodal loads appropriately placed along the deck axis, with an average interaxis of around 100 m.

Adopting the sum of the permanent load and accidental aerodynamic overloading as load combination, the following were obtained at mid-span of the deck :

- vertical arrow: -8.14 m
- horizontal displacement: 1.95 m
- rotation: not evaluated.

The only result available in the literature is the horizontal displacement: the order of magnitude of

Table 1 Comparison of the frequencies obtained by the FEM model and the frequencies obtained on the complete model in a wind gallery (Danish Maritime Institute)

	Wind Tunnel [Hz]	FEM [Hz]	[%]
Lateral symm.	0.0523	0.0524	0.19
Vertical symm.	0.0997	0.1060	5.94
Vertical antisymm.	0.1147	0.1141	0.53
Lateral antisymm.	0.1270	0.1220	4.10
Torsional symm.	0.2890	0.2929	1.33
Torsional antisymm.	0.3910	0.4006	2.40

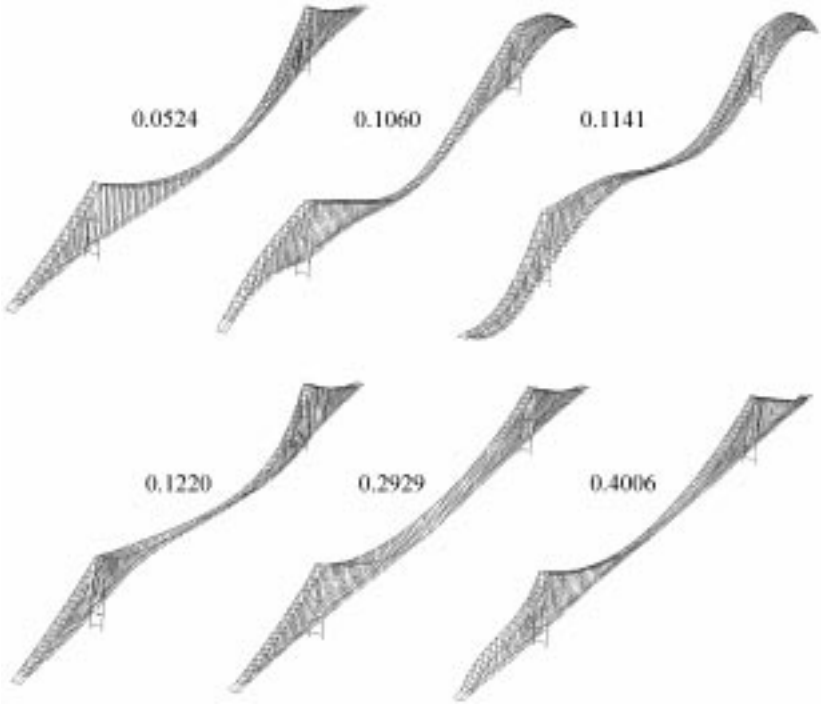

Fig. 3 Flexural and torsional modal forms

the error is ±2% (Larsen 1998a).

4.2. Analysis of aeroelastic stability

The aeroelastic stability analysis was preceded by the nonlinear static analysis necessary to determine the position of static equilibrium (defined as in Eq. 6) around which the motion occurs. To schematise the main cables prestressed beams were used in which the pre-loading static action is taken into account. This prestressing (3000 N per wire) was schematised by means of an equivalent thermal load. The final vertical arrow at mid-span is about 12m, in agreement with the real data supplied by the builder COINFRA S.p.A. (Sparatore 1998)

The Newton-Raphson algorithm was used to solve the problem, with updating of the matrices at each iteration.

The aeroelastic analysis showed an exponential trend, damped or amplified depending on whether the incident flow speed was lower or higher than the critical flutter speed (Fig. 4).

The analysis results agree with the experimental results obtained in the wind gallery and indicate a critical flutter speed of around 220 km/h, with a ratio value of structural damping in relation to the critical damping $\xi = c/c_{crit}$ equal to 0.025. The deck motion, in its flexural and torsional components, is represented in Fig. 5 for a wind speed well above the critical speed.

In order to precisely identify the critical flutter speed, various parameter-indexes were used to study the behaviour of the system (Fig. 6) :

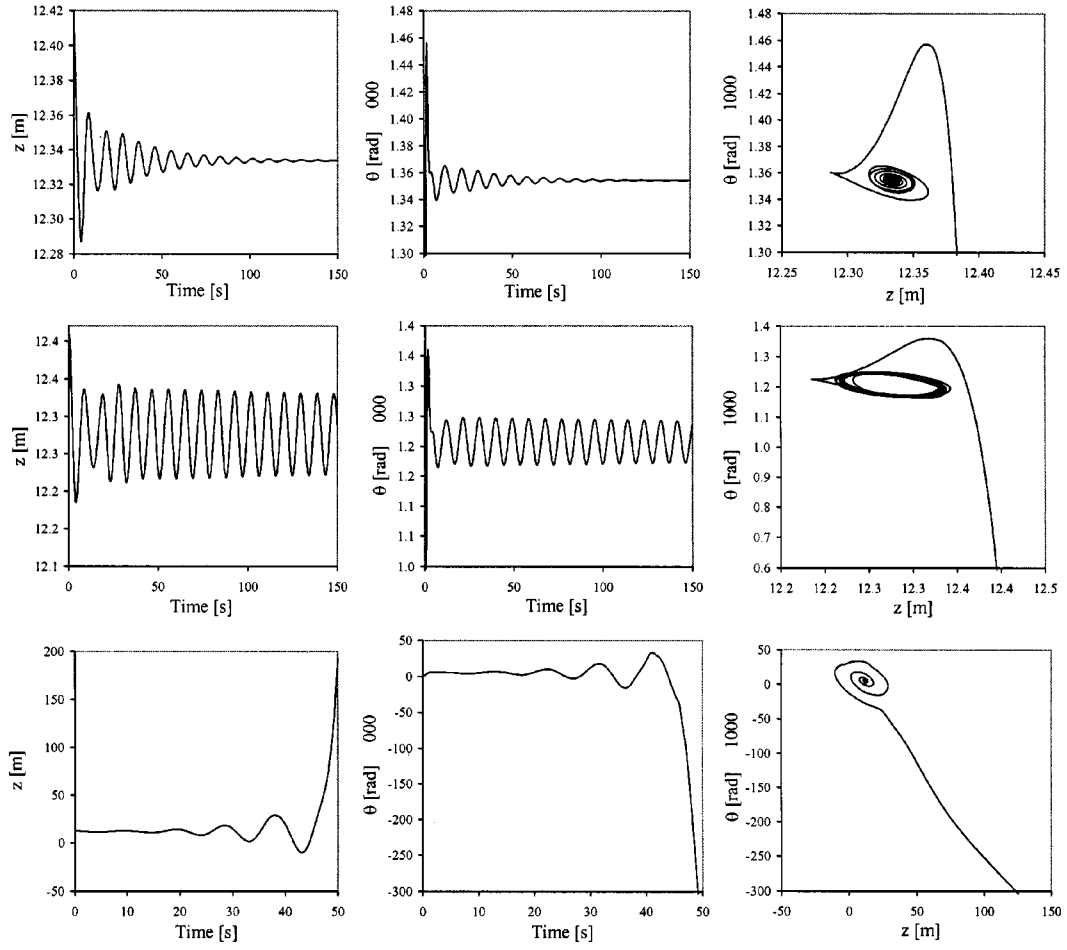

Fig. 4 Responses of the system for U = 41.7 m/s; U = 61.1 m/s; U = 97.2 m/s

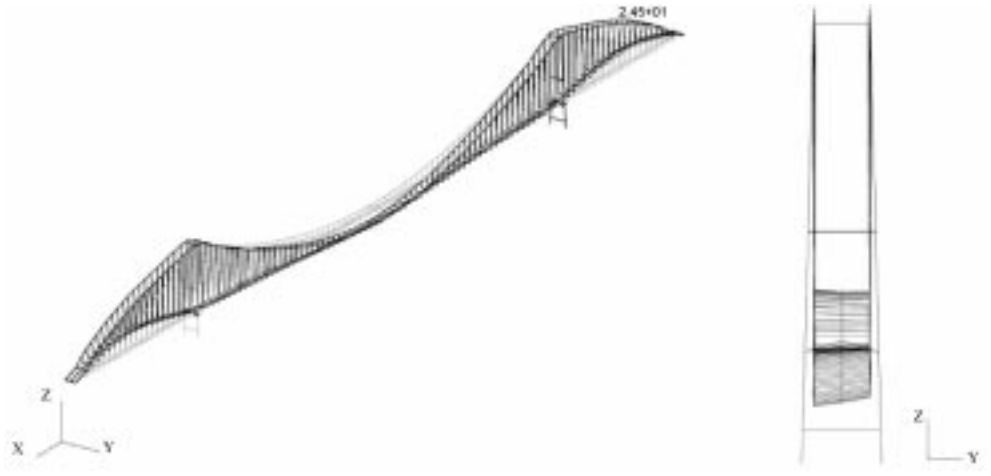

Fig. 5 Bridge deformation at instant t = 60s (wind speed = 97.2 m/s)

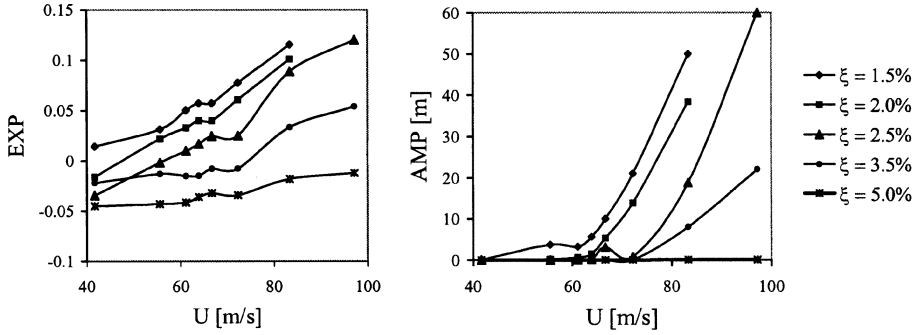

Fig. 6 Index parameters

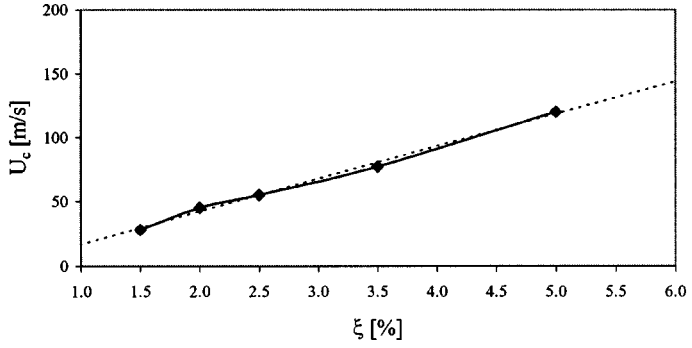

Fig. 7 Wind speed vs critical damping ratio

- Exponent (EXP) of the regression curve of the absolute value of the vertical oscillation at the mid-span or at the quarters, evaluated against the average displacement in time. The critical condition was identified by the zero value of this index; a negative value identifies stable behaviour (positive global damping); a positive value indicates an unstable situation (negative global damping).
- Average amplitude of the oscillations (AMP) at mid-span and at the quarters, evaluated at a fixed moment t^*. This index does not give an exact identification of the critical speed, but allows the extent of the structures displacements to be visually rated.

The motion of the structure is symmetrical, in complete agreement with the results obtained during the designing stage: analysis of the deck deformation shows the coupling of the first vertical mode and first torsional mode, both being symmetrical.

Having observed an accentuated dependence of the damping ratio ξ, a sensitivity analysis was done. The results obtained indicate a more or less linear trend of the critical speed with the varying of ξ (Fig. 7).

Analysis of the aeroelastic forces was done in relation to $t, \theta, \dot{\theta}, \dot{z}$. Analysing the contributions to the motion due to the various components of force separately, no form of instability appears for the usual speed intervals considered (Fig. 8). It is also noted that:

- the elements dependent on torsional rotation θ determine the average magnitude of the forces and of the displacements;

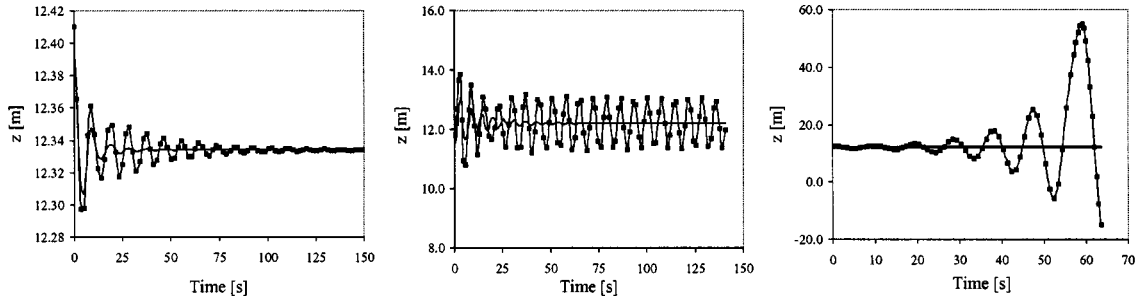

Fig. 8 Influence on motion of velocity elements

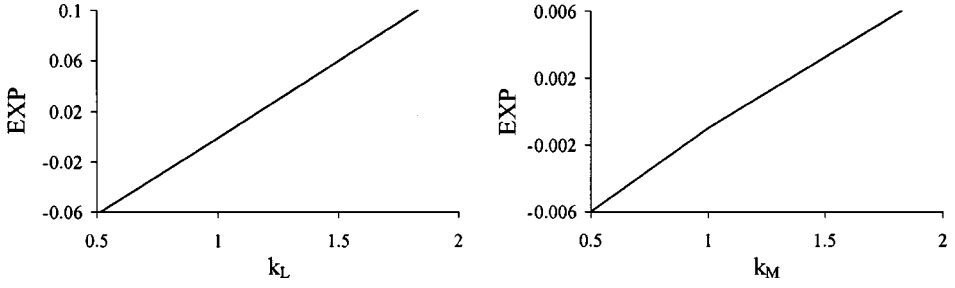

Fig. 9 Influence of aerodynamic coefficients $k_L=\{(\partial C_L/\partial\alpha)\}$ *e* $k_M=\{(\partial C_M/\partial\alpha)\}$

- the elements dependent on velocity $(\dot{\theta}, \dot{z})$, alone, cause no motion of the structure in the way they are defined;
- the elements dependent on rotation θ alone determine a stable response of the structure. Nevertheless, it is possible in this way to evaluate the phenomenon of the static torsional divergence, the critical speed of which depends exclusively on the torsional characteristics of the deck and on the bending action of the wind, and is in general much higher than the critical flutter speed:

$U_{DIV} = \sqrt{\dfrac{2k_\theta}{\left(\dfrac{\partial C_M}{\partial\alpha}\right)_{\alpha=\alpha_0}\rho B^2}}$. In conclusion it is noted that instability of the flutter type is caused by the contemporary dependence of the forces of the deck displacements and velocities.

Given that, in general, aerodynamic coefficients are not identifiable with high precision by means of a numerical fluid-dynamic analysis, a sensitivity analysis was conducted varying the value of the derivatives of these coefficients. The trend of the flutter index EXP, and therefore of the critical speed, results as almost linear (Fig. 9). Newmarks algorithm was used to solve the aeroelastic problem, updating the matrices at each iteration.

All the calculations were done using the MSC-Nastran calculating code on an Alpha Server Digital 2100 4/275 Mhz machine with 3 processors available and 256 MB of RAM. The time necessary for the solution of the preliminary nonlinear static analysis was around 10 seconds (user time), while the aeroelastic analyses required an average of 15 minutes (user time).

5. Conclusions

The analysis in the time domain, following the quasi-static formulation of the aerodynamic loads, results as being a reliable alternative to the usual analysis in the frequency domain (Section Model). It also allows the structural nonlinearities of the model to be considered and to follow the effective behaviour of the structure over time.

It has been shown that the uncertainty in determining the critical flutter speed derives, essentially, from the inexact estimate of the structural parameters. In particular, it is necessary to precisely evaluate the damping of the structure: variations in the ξ ratio of 10% determine errors in the flutter speed estimate in the order of 10% (±20 km/h). The model tests and frequency domain flutter analysis yield $U_{cr} \cong 70$ m/s which corresponds to a $\xi \cong 0.03$. The phenomenon is also slightly influenced by an inaccurate estimate of the aerodynamic coefficients: errors of 50% in these parameters lead to variations of 5% in the critical speed (±10 km/h).

References

Astiz, M. A. (1998), "Flutter stability of very long suspension bridges", *J. Bridge Eng.*, **3**(3), 132-139.

Bartoli, G., Borri, C. and Gusella, V. (1997), "On the influence of wind turbolence on bridge decks flutter", *Aspects in Modern Computational Structural Analysis*, Ed. by Meskouris & Wittek, Balkema, Rotterdam.

D'Asdia, P. and Sepe, V. (1997), "Aeroelastic instability of long span suspended bridges: a multi mode approach", *Proc. of the 2nd EACWE International Conference*, Genova, June.

Diana, G. and Cheli F. (1993), *Dinamica e vibrazione dei sistemi meccanici*, 2° Vol., UTET Libreria, Torino.

Diana, G., *et al.* (1998), "Aerodynamic design of very long-span suspension bridges", *IABSE Symposium*, Kobe, **79**, IABSE Reports.

Diana, G. and Falco, M. (1990), "Indagine analitico sperimentale su un ponte sospeso di grande luce soggetto all'azione del vento", *Atti del 1° Convegno Nazionale di Ingegneria del Vento IN-VENTO-90*, Firenze, October.

Dyrbye, C. and Hansen, S. D. (1997), *Wind Loads on Structures*, J. Wiley & Sons, Inc., Baffins Lane, Chichester.

Hansen, O. R. (1998), "Aerodynamics retrofits for the suspension bridge", *East Bridge*, Ed. by N. J. Gimsing, A/S Storebæltsforbindelsen, København, 383-384.

Larsen, A. (1998), "Aerodynamics investigation of the superstructure", *East Bridge*, Ed. by N. J. Gimsing, A/S Storebæltsforbindelsen, København, 78-85.

Larsen, A. (1998), "Computer simulation of wind-structure interaction in bridge aerodynamics", *Struct. Eng. Int.*, February, 105-111.

Larsen, A. (1998), "Wind tunnel tests, suspension bridge", *East Bridge*, Edited by Gimsing N. J., A/S Storebæltsforbindelsen, København, 187-192.

Larsen, A. and Jacobsen, A. S. (1992), "Aerodynamics design of the great belt east bridge", *Aerodynamics of Large Bridges*, Ed. by Larsen A., Balkema, Rotterdam, 269-283.

Li, Q. C. (1995), "Measuring flutter derivatives for bridge sectional models in water channel", *J. Eng. Mech.*, Jan., **121**(1), 90-101.

Miyata, T., Yamada, H. and Boonyapinyo, V. (1999), "Advanced aerodynamic analysis of suspension bridges by state-space approach", *J. Struct. Eng.*, Dic. , **125**(12), 1357-1366.

Pedersen, A. and Hauge, L. (1998), "Design of the suspension bridge", *East Bridge*, Ed. by Gimsing N. J., A/S Storebæltsforbindelsen, København, 167-186.

Reinhold, T. A., Brinch, M. and Damsgaard, A. (1992), "Wind tunnel tests for the Great Belt Link", *Aerodynamics of Large Bridges*, Ed. by Larsen A., Balkema, Rotterdam, 255-267.

Rolla, E., Sparatore, U. and Testa, A. (1997), "The construction of the storebælt east bridge superstructure (DK)", *Proc. of the 2nd EACWE International Conference*, Genova, June.

Scanlan, R.H. and Simiu, E. (1996[3]), *Wind Effects on Structures. Fundamentals and Application to Design*, J. Wiley & Sons, Inc., New York.

Sepe, V. and Augusti, L. (1999), "Unilateral behaviour of hangers and wind-induced oscillations of suspension bridges", *Proc. of the 6th Pan American Congress of Applied Mechanics PACAM VI*, Rio de Janeiro, January.
Sepe, V., Ciappi, E. and D'Asdia, P. (1996), "Instabilità aeroelastica multimodale di ponti sospesi", *Atti del 4° Convegno Nazionale di Ingegneria del Vento IN-VENTO-96*, Trieste, September.
Sparatore, U. (1998), "*La realizzazione del ponte sullo Storebælt*", COINFRA S.p.A. Seminar, Università di Genova - DISEG, Genova, 30 April.
Tanaka, H. (1998), "Aeroelastic stability of suspension bridges during erection", *Struct. Eng. Int.*, February, 118-123.
Tanaka, H. and Livesey, F. M. (1996), *Wind Tunnel Study of the Storebælt East Suspension Bridge in Its Early Deck Erection Phases*, Danish Maritime Institute, 15 November.
Zasso, A. (1996), "Flutter derivatives: advantages of a new representation convention", *J. Wind Eng. Ind. Aerod.*, **60**, 35-47.

CC